Multi-wavelength Signatures of a Coronal Mass Ejection

N. Gopalswamy*
NASA Goddard Space Flight Center, Greenbelt, MD 20771, USA
E-mail: gopals@fugee.gsfc.nasa.gov
S. Yashiro
Department of Astronomy, University of Tokyo, Tokyo, Japan
M. L. Kaiser, and B. J. Thompson
NASA Goddard Space Flight Center, Greenbelt, MD 20771, USA
and
S. Plunkett
USRA, Naval Research Laboratory, Washington DC 20375, USA

Abstract

We report on the near-surface and outer coronal manifestations of the 1998 January 25 coronal mass ejection (CME) using white light, EUV, X-ray and hectometric radio data which reveal the three dimensional structure and long term evolution of the CME. We find that (i) the substructures of the CME (prominence core, cavity, frontal structure and the arcade formation) are clearly observed in X-ray and EUV wavelengths. (ii) The filament heats up early on and is observed as a backbone in X-rays. (iii) The filament also expands considerably as it erupts. (iv) The CME is observed through direct leading edge signature as well as through dimming process in X-rays and in EUV.

Key words: Sun: CMEs — Sun: prominence Eruptions — Sun: Radio bursts

1. Introduction

Lack of information close to the solar surface has been a major drawback in making progress on the understanding of the origin of coronal mass ejections (CMEs). Since white light coronagraphs have to use an occulting disk, we have to resort to X-ray, EUV and microwave observations to study the near-surface manifestations of CMEs (Gopalswamy, 1999; Gopalswamy et al, 1997). After the advent of the Yohkoh, SOHO and Wind missions and the Nobeyama radioheliograph, we have a wealth of additional information that can clarify a number of issues related to the origin of CMEs. For instance, soft X-ray dimming (Hudson and Webb, 1997; Gopalswamy and Hanaoka, 1998), EIT waves and EUV dimming (Thompson et al 1998) have demonstrated the large-scale nature of the CME eruption. In this paper, we describe the 1998 January 25 CME event which was observed in its entirety by a number of instruments.

2. Observational Results

The data set consists of (i) white light observations of the CME from the SOHO Large Angle Spectrometric Coronagraph (LASCO, Brueckner et al, 1995) which can track CMEs from close to the Sun to 30 $R_\odot$, (ii) SOHO Extreme Ultraviolet Imaging Telescope (EIT, Delaboudinière et al, 1995) observations of filament eruption, coronal dimming and arcade formation, (iii) Yohkoh Soft X-ray Telescope (SXT, Tsuneta et al, 1991) observations of heated filament and frontal structure and X-ray dimming, (iii) Wind Radio and Plasma Waves (WAVES, Bougeret et al, 1995) observation of a Type II radio burst and herringbone structure. The event originated to the east of the disk center (N24 E27) as a filament eruption associated with a H-α subflare and a GOES C1.1 X-ray flare (Solar Geophysical Data, February 1998).

Figure 1 shows the filament just before its eruption as observed by EIT at 304 Å (marked F). Also shown are SXT images at several times. Note that the filament brightens in X-rays (arrow in the 14:03 UT image) and then

* NAS/NRC Senior Research Associate.

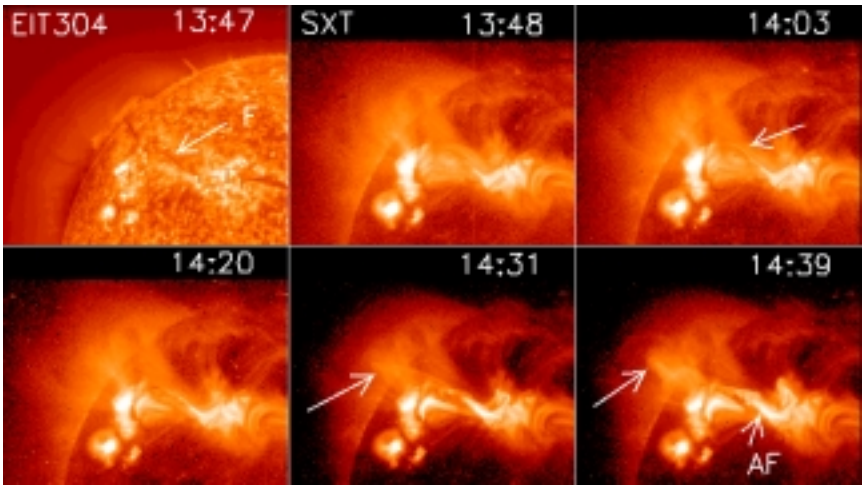

Fig. 1.. EIT image at 13:47 UT and a series of SXT images showing the early the evolution of the eruptive event. F is the filament that heated and erupted. Initial X-ray brightening along the filament can be seen in the 14:03 UT image. The ejected prominence is indicated by arrows in the 14:31 and 14:39 UT images. AF is the arcade formation in X-rays. North is to the top and east is to the left.

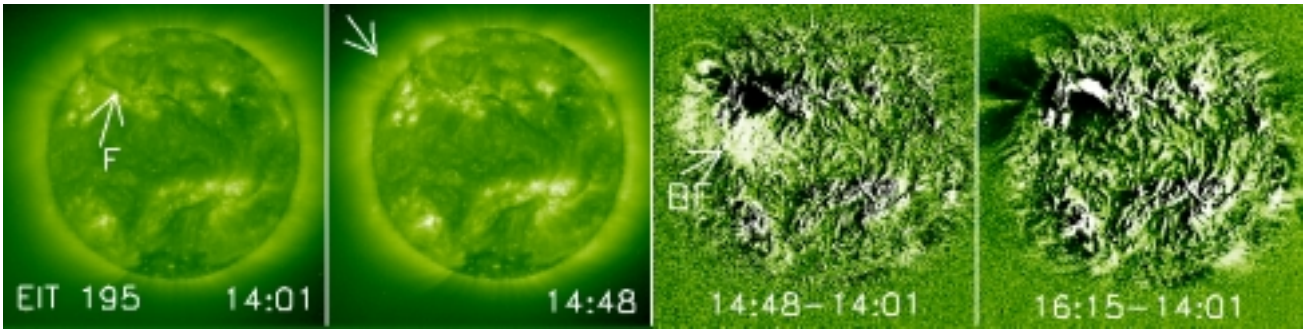

Fig. 2.. Direct (first two) and difference (last two) images from SOHO/EIT showing the near-surface manifestations of the 1998 January 25 CME. The filament marked F at 14:01 UT erupted and can be seen above the limb at 14:48 UT (arrow). formation. The difference image at 14:48 shows this filament as the core of a section of the CME with three part structure and a bright front (BF) at the outskirts of the EUV dimming region. The difference image at 16:15 UT shows the large scale nature of the dimming region and a bright arcade formation at the initial location of the filament.

is ejected (speed $\sim$ 120 km s^{-1}) above the limb as pointed by arrows in the 14:31 and 14:39 images. Following the filament ejection was an arcade formation (AF) at the initial location of the filament. Two smaller arcades can also be seen on either side of AF suggesting the possibility of multiple neutral lines involved in the eruptive event (Webb et al, 1998; Gopalswamy et al, 1998). Figure 2 shows the evolution of the region of eruption as observed by EIT at 195 Å from 14:01 to 16:15 UT in direct and difference images. The difference images show extensive EUV dimming on either side of the neutral line. There is also an EUV brightening (marked BF) which brackets the dimming on the southern side. The ejected filament can be clearly seen above the northeast limb in the difference image at 14:48 UT with an overlying coronal structure. This is very similar to the three-part structure (filament, void and frontal) seen in X-rays (see also the 14:39 UT image in Fig. 1). Note that the ejected prominence (heated plasmoid) appears larger in X-rays than in EUV, because of different temperature responses of EIT and SXT. The difference image at 16:15 UT shows the arcade formation along the neutral line and the extensive depletion of EUV emission from a large region on and above the disk.

A CME was first detected by the C2 coronagraph of SOHO/LASCO at 15:26 UT above the northeast limb as a bright arcade. Fig. 3 shows four white light running difference images of the CME. The CME eventually became a halo event, with some of the faint features moving to the west in projection (pointed to by arrow marks). By

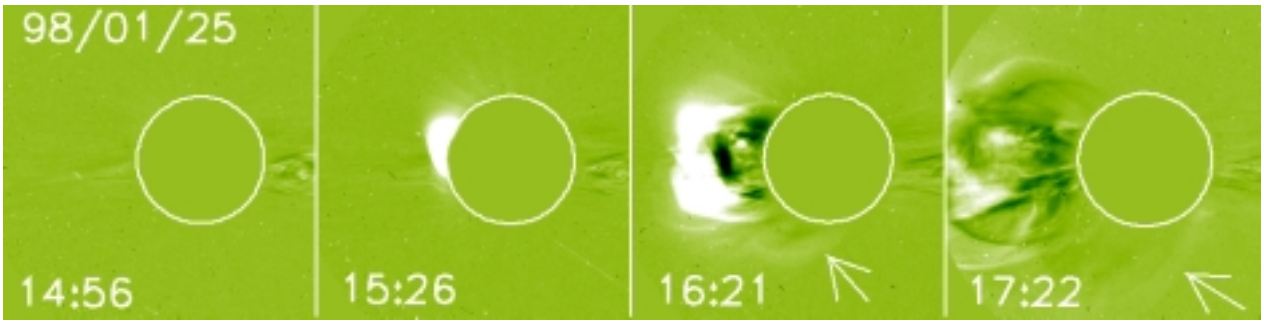

Fig. 3.. SOHO/LASCO halo CME observed by the C2 coronagraph. The arrows point to a faint feature that extends all the way to the west limb. The white circle represents the occulting disk of the C2 coronagraph (radius $\sim 2\ R_\odot$).

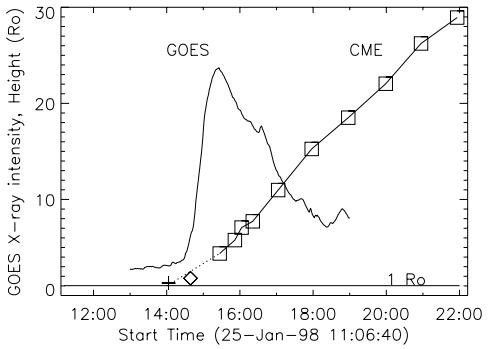

Fig. 4.. GOES plot showing the weak X-ray activity. The C1.1 flare at 14:29 UT (peak: 15:12 UT, end: 17:00 UT) represents the arcade formation. In H-α, the event was observed as a subflare starting, peaking and ending at 15:30, 15:30 and 15:38 UT respectively. The CME height-time plot is also shown (squares represent CME heights). The X-ray flux is divided by 5×10^{-8} W m^{-2}. The X-ray (plus) and EUV (diamond) measurements of the leading edge of the CME are also shown on the height-time plot.

measuring the height of the CME leading edge in Fig. 3, we estimated a speed of ~ 700 km s^{-1} in projection. The height-time plot of the CME is shown in Fig. 4 along with the GOES X-ray plot. As we saw in the SXT images, the X-ray emission is due to the filament brightening and arcade formation, with no impulsive flare involved.

No metric radio emission was observed before 16:18 UT. However, the WAVES experiment observed a radio event starting from 15:12 UT. The emission consisted of fast drifting bursts (Type III like) and a slow drifting (type II) burst. The slow drifting bursts are thought to be due to MHD shock waves in the corona, while the fast-drifting type III bursts are created by relativistic electron beams. The radio emission must have started at frequencies higher than 14 MHz (upper frequency limit of WAVES observations). Since there was no radio emission down to 25 MHz from ground based observations, we think that the type II emission started somewhere between 14 and 25 MHz. Note that the CME appeared above the C2 occulting disk just about this time and must have caused the type II radio burst. The fast drifting bursts are probably herringbones which are type III-like bursts produced by electron beams escaping from the type II shock.

3. Discussion and Conclusions

The eruption is very complex with loops of different temperatures present between the leading edge and the prominence core. The prominence heats up and expands very early in the event. The different appearance of the prominence in X-rays and EUV is probably due to the temperature structure of the heated prominence (or plasmoid) and the temperature response of the two instruments. The appearance of the white light CME at a heliocentric distance of 3 $R_\odot$ at 15:26 UT clearly precedes the H-α flare onset (on the surface) at 15:30 UT. The CME trajectory

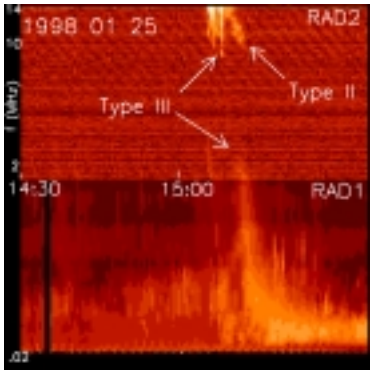

Fig. 5.. Combined dynamic spectrum from Wind/WAVES RAD2 (14–1 MHz) and RAD1 (1–.02 MHz). The vertical features are type III bursts; slanted feature is the type II burst.

from white light data is consistent with the X-ray and EUV observations. If the EUV bright front (14:48 UT) is considered as the leading edge of a cylindrical CME overlying the neutral line, we can estimate its height at 14:48 UT as 0.7 $R_\odot$. This is also consistent with the height (0.3 $R_\odot$) of the X-ray frontal structure overlying the hot plasmoid (see Fig. 1).

The type II burst seems to be due to a shock driven by the CME at large heights. Note that the large height of the type II burst is inferred from the low starting frequency but we do not know the actual height without positional information on type II bursts. It is somewhat puzzling that the type II is short-lived. The start of the lower frequency herringbone bursts with no backbone emission suggests that the observed type II emission is at the second harmonic of the local plasma frequency. i.e., the emission originates from coronal levels where the local plasma frequency is about 8 MHz (plasma density less than about 8×10^5 cm^{-3}). This means the shock formed at very large distances (at least several solar radii) from the sun.

The arcade formation is observed at both X-ray and EUV wavelengths. In addition to the main arcade formation over the initial location of the filament, there were two small arcades that formed on either side of it. There may be other neutral lines involved on either side of the arcade formation. These will be explored further and reported elsewhere. The EIT dimming is somewhat symmetrical on either side of the neutral line over which the main post-eruption arcade formed. Clear expansion of linear features could be seen from the dimming regions when the images are played as movies. These are probably structures belonging to the CME base.

Part of this work was performed during the 1998 SOHO-Yohkoh Coordinated Data Analysis Workshop in ISAS, Japan. NG was upported by NASA grant NAG-5-6139 and by NSF through a subcontract from the University of Maryland, College Park. NG thanks the organizers of the symposium for travel support.

References

Bougeret, J.-L. et al. 1995, Space Sci. Rev., 71, 237
Brueckner, G. E., et al. 1995, Solar Phys., 162, 357
Delaboudiniére, J. et al. 1995, Solar Phys., 162, 291
Gopalswamy, N. 1999, this volume
Gopalswamy, N. Kundu, M. R., Manoharan, P. K., Raoult, A., Nitta, N. and Zarka, P. 1997, ApJ, 486, 1036
Gopalswamy, N. and Hanaoka, Y. 1998, ApJL, 498, L179
Gopalswamy, N., Hanaoka, Y. and Lemen, J. R. 1998, in 'New Perspectives on Solar Prominences,' D. F. Webb, D. Rust and B. Schmieder, (eds.), ASP Conf. ser. 150, p. 358
Hanaoka, Y. et al. 1994, PASJ, 46, 205
Hudson, H. S. and Webb, D. F. 1997 in 'Coronal Mass Ejections', N. Crooker, J. A. Joselyn and J. Feynman (eds.), AGU, Washington DC, p. 27
Thompson, B. J., Plunkett, S. P., Gurman, J. B., Newmark, J. S., St. Cyr, O. C. and Michels, D. J. 1998, Geophys. Res. Lett., 25, 2465
Tsuneta, S. et al. 1991, Solar Phys. 136, 37
Webb, D. F., Kahler, S. W., McIntosh, P. S., and Klimchuck, J. A. 1998, J. Geophys. Res., 102, 24161